Article

Arsenates of Divalent Metals Comprising Arsenic Acid—An Update

Matthias Weil

Institute for Chemical Technologies and Analytics, Division of Structural Chemistry, TU Wien, Getreidemarkt 9/164-SC, A-1060 Vienna, Austria; Matthias.Weil@tuwien.ac.at

Received: 6 September 2019; Accepted: 1 October 2019; Published: 9 October 2019

Abstract: Divalent metal oxidoarsenates(V) with compositions $M(H_2AsO_4)_2(H_3AsO_4)_2$ (M = Mg, Mn, Co, Ni), $M(HAsO_4)(H_3AsO_4)(H_2O)_{0.5}$ (M = Mn, Cd) and $Zn(HAsO_4)(H_3AsO_4)$ were obtained from solutions containing an excess of arsenic acid. Single crystal X-ray diffraction revealed isotypism of the $M(H_2AsO_4)_2(H_3AsO_4)_2$ (M = Mg, Mn, Co, Ni) structures with the known Cu and Zn members of this series whereas $M(HAsO_4)(H_3AsO_4)(H_2O)_{0.5}$ (M = Mn, Cd) and $Zn(HAsO_4)(H_3AsO_4)$ crystallize in novel structure types. The two isotypic $M(HAsO_4)(H_3AsO_4)(H_2O)_{0.5}$ (M = Mn, Cd) structures are closely related with that of $Zn(HAsO_4)(H_3AsO_4)$. Both comprise undulating centrosymmetric ${}^{1}_{\infty}[MO_{4/2}O_{2/1}]$ chains that share corners with $HAsO_4{}^{2-}$ tetrahedra and H_3AsO_4 tetrahedra to build up layers extending along (001). Intermediate water molecules (occupancy 0.5) link adjacent layers in the water-containing compound whereas the linkage in the Zn-compound is mediated by weak hydrogen bonding interactions between the layers. Results of a quantitative comparison between all known structures of the $M(H_2XO_4)_2(H_3XO_4)_2$ (M = Mg, Mn, Co, Ni, Cu, Zn; X = P, As) series as well as between the two $M(HAsO_4)(H_3AsO_4)(H_2O)_{0.5}$ (M = Mn, Cd) structures are presented.

Keywords: arsenates; arsenic acid; crystal structure; hydrogen bonding; isotypism; structure comparison

---

1. Introduction

Inorganic phosphates or arsenates of divalent metals with the corresponding free acid as structure units are restricted to a handful of compounds. Most probably, $Zn(H_2PO_4)_2(H_3PO_4)_2$ was one of the first of such phases ever reported [1], however without giving structural details at that time. More than three decades later, the crystal structure of $Co(H_2PO_4)_2(H_3PO_4)_2$ was determined, providing full details of the hydrogen bonding scheme in the structure [2], and later reported as being isotypic with the zinc phase [3]. Approximately at the same time, the first arsenate phase $CdH_{10}(AsO_4)_4$ (or $Cd(H_2AsO_4)_2(H_3AsO_4)_2$) was structurally determined but without localization of H positions [4], claiming isotypism of the Cd member with structures of the series $M(H_2AsO_4)_2(H_3AsO_4)_2$ (M = Mg, Mn, Co, Ni, Cu and Zn). However, the isotypic relationship between $CdH_{10}(AsO_4)_4$ and the $M(H_2AsO_4)_2(H_3AsO_4)_2$ series was questioned some years later during structure determination of the copper(II) phase $Cu(H_2AsO_4)_2(H_3AsO_4)_2$ [5]. Next to the previously reported Zn representative [6], the two structures are the only members of the $M(H_2AsO_4)_2(H_3AsO_4)_2$ series for which detailed structure data, including H atom positions, have been determined so far.

The current study was devoted to crystallize other members of the $M(H_2AsO_4)_2(H_3AsO_4)_2$ series (M = Mg, Mn, Co, Ni) to achieve detailed structural data from single crystal X-ray diffraction with the purpose to prove isotypism and to quantify structural relationships between them with the aid of the program *compstru* [7]. Next to the four $M(H_2AsO_4)_2(H_3AsO_4)_2$ (M = Mg, Mn, Co, Ni) members, three other arsenates with additional arsenic acid moieties, *viz.* $M(HAsO_4)(H_3AsO_4)(H_2O)_{0.5}$ (M = Mn, Cd) and $Zn(HAsO_4)(H_3AsO_4)$, were obtained during this study for the first time and were structurally characterized by single crystal X-ray diffraction.

2. Results and Discussion

2.1. Crystal Structures of the $M(H_2AsO_4)_2(H_3AsO_4)_2$ Series (M = Mg, Mn, Co, Ni)

The $M(H_2AsO_4)_2(H_3AsO_4)_2$ (M = Mg, Mn, Co, Ni) crystal structures are isotypic with $Co(H_2PO_4)_2(H_3PO_4)_2$ [2], $Cu(H_2AsO_4)_2(H_3AsO_4)_2$ [5] and $Zn(H_2AsO_4)_2(H_3AsO_4)_2$ [6]. Since for all of the latter compounds a detailed structure description has already been given, only the most important features of this structure type are briefly depicted here.

The divalent metal cations M are located on an inversion center (Wyckoff position 1*a*). They are surrounded by six oxygen atoms in the form of a slightly distorted octahedron. Four oxygen atoms (O7, O5 and their symmetry-related counterparts) belong to the O atoms of the $H_2AsO_4^-$ group (As2) and make up the equatorial plane, while the H_3AsO_4 group (As1) provides two oxygen atoms (O3 and its symmetry-related counterpart) in axial positions with the longest M–O distance in the octahedron (Figure 1; Table 1).

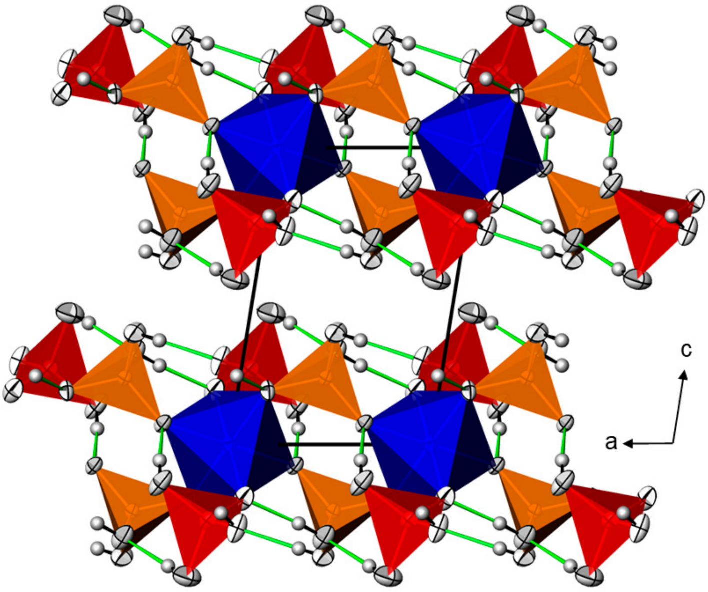

Figure 1. Representative for the $M(H_2XO_4)_2(H_3XO_4)_2$ series, the crystal structure of $Mn(H_2AsO_4)_2(H_3AsO_4)_2$ is given in a projection along ⟨010⟩. Displacement ellipsoids are drawn at the 90% probability level. $H_2AsO_4^-$ tetrahedra (As2) are orange, H_3AsO_4 tetrahedra (As1) are red, MnO_6 octahedra are blue; H atoms are displayed as grey spheres of arbitrary radius. O···H hydrogen bonds are shown as green lines.

Individual M–O bond lengths and their mean values are typical for the corresponding metal cation. In accordance with the largest ionic radius of Mn of all four M^{II} cations (M = Mg, Mn, Co, Ni) [8], Mn exhibits the longest M–O bonds. Neighboring metal cations are linked into chains along ⟨100⟩ by bridging $H_2AsO_4^-$ groups; the H_3AsO_4 group is attached to the chains and has no bridging character. An intricate network of strong to medium-strong hydrogen bonds (Table 2) connects the chains into layers extending along (010) (Figure 1) whereby all O atoms that do not bond to the M cations carry a hydrogen atom. Hydrogen bonds of remarkable strengths between the layers do not exist.

Table 1. Selected bond lengths/Å, angles/° with estimated standard deviations in parentheses, and bond valence parameters (BVS)/valence units. Averaged values (av.) are given in the last line of each column.

$Mn(HAsO_4)(H_3AsO_4)(H_2O)_{0.5}$					**$Cd(HAsO_4)(H_3AsO_4)(H_2O)_{0.5}$**					**$Zn(HAsO_4)(H_3AsO_4)$**				
Mn1	–	O3	2.149(2)		Cd1	–	O3	2.242(3)		Zn1	–	O3	2.031(3)	
	–	O5	2.162(3)			–	O5	2.253(4)			–	O7	2.048(3)	
	–	O7	2.186(3)			–	O7	2.273(3)			–	O2	2.123(4)	
	–	O7	2.202(3)			–	O7	2.307(3)			–	O5	2.127(4)	
	–	O2	2.229(3)			–	O2	2.307(3)			–	O7	2.180(4)	
	–	O3	2.229(3)			–	O3	2.314(3)			–	O3	2.204(4)	
		av.	2.19				av.	2.28				av.	2.12	
As1	–	O7	1.666(3)		As1	–	O7	1.663(3)		As1	–	O7	1.669(3)	
	–	O3	1.673(3)			–	O3	1.672(3)			–	O3	1.673(3)	
	–	O2	1.698(3)			–	O2	1.696(3)			–	O2	1.690(4)	
	–	O1	1.708(3)			–	O1	1.714(4)			–	O1	1.710(4)	
		av.	1.686				av.	1.686				av.	1.689	
As2	–	O5	1.654(3)		As2	–	O5	1.649(4)		As2	–	O5	1.668(4)	
	–	O4	1.666(3)			–	O4	1.670(4)			–	O4	1.673(4)	
	–	O6	1.692(5)			–	O6	1.686(7)			–	O8	1.687(4)	
	–	O8	1.705(5)			–	O8	1.702(6)			–	O6	1.698(5)	
		av.	1.680				av.	1.677				av.	1.682	
BVS														
Mn1 2.03, As1 5.01, As2 5.11, O1 1.18, O2 1.52, O3 1.98, O4 1.33, O5 1.73, O6 1.23, O7 2.00, O8 1.19.					Cd1 2.16, As1 5.01, As2 5.15, O1 1.16, O2 1.55, O3 2.03, O4 1.31, O5 1.78, O6 1.25, O7 2.04, O8 1.20.					Zn1 1.98, As1 5.02, As2 5.07, O1 1.17, O2 1.56, O3 1.97 O4 1.30, O5 1.64, O6 1.21, O7 1.99, O8 1.25.				
$Mg(H_2AsO_4)_2(H_3AsO_4)_2$					**$Mn(H_2AsO_4)_2(H_3AsO_4)_2$**					**$Co(H_2AsO_4)_2(H_3AsO_4)_2$**				
Mg1	–	O7	2.0680(13)	2×	Mn1	–	O7	2.1629(9)	2×	Co1	–	O7	2.050(3)	2×
	–	O5	2.0853(14)	2×		–	O5	2.1707(9)	2×		–	O5	2.146(3)	2×
	–	O3	2.1205(14)	2×		–	O3	2.2120(11)	2×		–	O3	2.146(4)	2×
		av.	2.09				av.	2.18				av.	2.11	
As1	–	O3	1.6484(14)		As1	–	O3	1.6458(10)		As1	–	O3	1.650(3)	
	–	O1	1.6852(14)			–	O1	1.6831(10)			–	O1	1.687(3)	
	–	O4	1.6983(16)			–	O4	1.6983(11)			–	O4	1.696(3)	
	–	O2	1.7096(15)			–	O2	1.7037(12)			–	O2	1.711(4)	
		av.	1.685				av.	1.683				av.	1.686	
As2	–	O5	1.6562(15)		As2	–	O5	1.6552(9)		As2	–	O5	1.663(3)	
	–	O7	1.6579(14)			–	O7	1.6561(9)			–	O7	1.665(3)	
	–	O6	1.7119(14)			–	O6	1.7076(11)			–	O6	1.709(4)	
	–	O8	1.7161(15)			–	O8	1.7131(11)			–	O8	1.717(4)	
		av.	1.686				av.	1.683				av.	1.689	
$Ni(H_2AsO_4)_2(H_3AsO_4)_2$														
Ni1	–	O7	2.037(3)	2×										
	–	O5	2.097(3)	2×										
	–	O3	2.117(3)	2×										
		av.	2.08											
As1	–	O3	1.644(3)											
	–	O1	1.694(3)											
	–	O4	1.696(3)											
	–	O2	1.712(3)											
		av.	1.689											
As2	–	O5	1.656(3)											
	–	O7	1.664(3)											
	–	O6	1.713(3)											
	–	O8	1.713(3)											
		av.	1.687											

Table 2. Details of the hydrogen bonding geometry/Å, °.

D	H	*A*	*D*–H	H···*A*	*D*···*A*	*D*–H···*A*
$Mg(H_2AsO_4)_2(H_3AsO_4)_2$						
O2	H1	O8	0.890(10)	1.918(18)	2.769(2)	160(4)
O1	H2	O7	0.898(10)	1.620(11)	2.517(2)	174(4)
O4	H3	O5	0.895(10)	1.758(14)	2.634(2)	167(4)
O6	H4	O1	0.884(10)	1.96(2)	2.760(2)	149(4)
O8	H5	O3	0.893(10)	1.686(11)	2.577(2)	174(4)
$Mn(H_2AsO_4)_2(H_3AsO_4)_2$						
O2	H1	O8	0.890(10)	1.921(11)	2.8018(16)	170(3)
O1	H2	O7	0.898(10)	1.654(13)	2.5358(14)	167(4)
O4	H3	O5	0.895(10)	1.759(12)	2.6452(15)	170(3)
O6	H4	O1	0.884(10)	1.932(12)	2.7968(14)	166(3)
O8	H5	O3	0.893(10)	1.723(13)	2.6007(14)	167(4)
$Co(H_2AsO_4)_2(H_3AsO_4)_2$						
O2	H1	O8	0.898(10)	1.94(3)	2.812(5)	163(8)
O1	H2	O7	0.901(10)	1.69(3)	2.564(5)	162(8)
O4	H3	O5	0.898(10)	1.75(3)	2.616(5)	162(7)
O6	H4	O1	0.896(10)	1.94(3)	2.799(4)	159(7)
O8	H5	O3	0.899(10)	1.71(2)	2.592(5)	167(8)
$Ni(H_2AsO_4)_2(H_3AsO_4)_2$						
O2	H1	O8	0.897(10)	1.92(3)	2.762(4)	155(6)
O1	H2	O7	0.898(10)	1.629(17)	2.516(4)	169(6)
O4	H3	O5	0.899(10)	1.75(3)	2.610(4)	159(6)
O6	H4	O1	0.897(10)	1.90(2)	2.755(4)	159(6)
O8	H5	O3	0.900(10)	1.658(14)	2.553(4)	172(7)
$Mn(HAsO_4)(H_3AsO_4)(H_2O)_{0.5}$						
O1		O5			2.635(4)	
O4		O2			2.458(5)	
O8		O4			2.633(6)	
O6		OW			2.61(2)	
O8		OW			2.64(2)	
OW		O8			2.90(2)	
OW		O6			2.92(2)	
$Cd(HAsO_4)(H_3AsO_4)(H_2O)_{0.5}$						
O1		O5			2.625(5)	
O4		O2			2.470(5)	
O8		O4			2.670(7)	
O6		OW			2.75(4)	
O8		OW			2.60(4)	
OW		O6			2.84(4)	
OW		O8			2.94(4)	
$Zn(HAsO_4)(H_3AsO_4)$						
O1		O5			2.610(6)	
O4		O2			2.429(6)	
O8		O4			2.666(6)	
O6		O4			2.962(7)	
O6		O4			3.071(7)	

2.2. Crystal Structures of M(HAsO$_4$)(H$_3$AsO$_4$)(H$_2$O)$_{0.5}$ (M = Mn, Cd) and Zn(HAsO$_4$)(H$_3$AsO$_4$)

The *M*$(HAsO_4)(H_3AsO_4)(H_2O)_{0.5}$ (*M* = Mn, Cd) and $Zn(HAsO_4)(H_3AsO_4)$ compounds appeared as the first crystallization products in the strongly acidic aqueous solutions and subsequently converted into the *M*$(H_2AsO_4)_2(H_3AsO_4)_2$ compounds after a few days, or to koritnigite ($ZnHAsO_4{\cdot}H_2O$) for the Zn compound. This behavior indicates a dynamic equilibrium between the double and single deprotonated $HAsO_4^{2-}$ and $H_2AsO_4^-$ anions and fully protonated H_3AsO_4. Apparently, in the first crystallization stage the less acidic *M*$(HAsO_4)(H_3AsO_4)(H_2O)_{0.5}$ (*M* = Mn, Cd) compounds form, and in the subsequent crystallization stage the higher acidic *M*$(H_2AsO_4)_2(H_3AsO_4)_2$ compounds. This behavior, however, is reversed for the Zn compounds where the less acidic phase $ZnHAsO_4 \cdot H_2O$ formed as the second crystallization product. Therefore, a clear trend cannot be noticed for these systems.

The two $M(HAsO_4)(H_3AsO_4)(H_2O)_{0.5}$ (M = Mn, Cd) crystal structures are isotypic. All atoms in the asymmetric unit are located on general positions. The M^{II} cations exhibit a considerably distorted octahedral coordination environment, with bond lengths between 2.14 and 2.23 Å in the Mn structure and between 2.24 and 2.32 Å in the Cd structure. In contrast to the $M(H_2AsO_4)_2(H_3AsO_4)_2$ structure type (M:As ratio = 4) where isolated MO_6 octahedra are linked by bridging dihydrogenarsenate groups into chains, the MO_6 octahedra in the $M(HAsO_4)(H_3AsO_4)(H_2O)_{0.5}$ structure type (M:As ratio 1:2) share edges under formation of undulating centrosymmetric ${}^{1}_{\infty}[MO_{4/2}O_{2/1}]$ chains running parallel (010). As expected, the Cd–O bonds are longer (on average about 0.09 Å) than the Mn–O bonds. $As1O_4$ tetrahedra share two corners with the M cation within the ${}^{1}_{\infty}[MO_{4/2}O_{2/1}]$ chain, and one corner with an M cation in an adjacent chain, thus bridging the chains into layers extending along (001). $As2O_4$ tetrahedra share only one O atom with the chain and make up the outer boundary of the layers. A disordered water molecule is situated approximately at $c/2$ and links neighboring layers along (001) (Figure 2a).

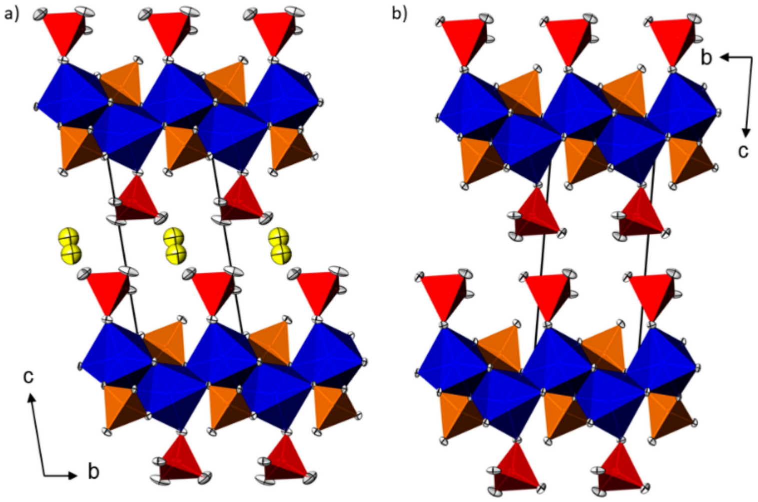

Figure 2. (**a**) Representative for the two $M(HAsO_4)(H_3AsO_4)(H_2O)_{0.5}$ (M = Mn, Cd) compounds, the crystal structure of $Mn(H_2\mathit{As}O_4)_2(H_3AsO_4)_2$ is given in a projection along (100); (**b**) the crystal structure of $Zn(HAsO_4)(H_3AsO_4)$ in a projection along (100). Displacement ellipsoids are drawn at the 50% probability level. $HAsO_4{}^{2-}$ tetrahedra (As1) are orange, H_3AsO_4 tetrahedra (As2) are red, and MO_6 octahedra are blue. Water molecules are yellow, with both possible positions (occupancy 0.5) shown.

The crystal structure of $Zn(HAsO_4)(H_3AsO_4)$ is closely related to that of the water-containing layered crystal structure type of $M(HAsO_4)(H_3AsO_4)(H_2O)_{0.5}$. A relation between the crystal structures of $M(HAsO_4)(H_3AsO_4)(H_2O)_{0.5}$ and $Zn(HAsO_4)(H_3AsO_4)$ is apparent from the similar topological arrangement of structure units (Figure 2) and similar lengths of the unit cell axes, with $a \approx 5.0$, $b \approx 5.4$, $c \approx 13.4$ Å. However, the unit cell angles in the two types of structures differ considerably, with all three angles <90° for the Zn structure and all three angles >90° in the Mn and Cd structures. Since it is not possible to transform one of the unit cells into a setting that has comparable axes *and* angles (all >90° or all <90°) to the other unit cell, the given reduced cells (Table 3) with $a \leq b \leq$ c and either with all angles >90° or <90° were used.

The general set-up within the (001) layers in the two crystal structures is the same. Since Zn has a smaller ionic radius in comparison with Mn and Cd [8], the Zn–O distances are the shortest in the ${}^{1}_{\infty}[MO_{4/2}O_{2/1}]$ chains. The main difference between the crystal structures is related to the missing water molecule in $Zn(HAsO_4)(H_3AsO_4)$. Here adjacent layers are directly stacked along [001] (Figure 2b).

Table 3. Details of X-ray data collections and crystal structure refinements.

Compound	**$Mn(HAsO_4)$-$(H_3AsO_4)(H_2O)_{0.5}$**	**$Cd(HAsO_4)(H_3AsO_4)$-$(H_2O)_{0.5}$**	**$Zn(HAsO_4)$-(H_3AsO_4)**	**$Mg(H_2AsO_4)_2$-$(H_3AsO_4)_2$**	**$Mn(H_2AsO_4)_2$-$(H_3AsO_4)_2$**	**$Co(H_2AsO_4)_2$-$(H_3AsO_4)_2$**	**$Ni(H_2AsO_4)_2$-$(H_3AsO_4)_2$**
M_R	345.82	403.28	347.24	590.07	620.70	624.69	624.47
Temp./°C	23	23	23	–173	23	23	23
Radiation; λ/Å	— Mo Kα; 0.71073 —						
Diffractometer	APEXII CCD	SMART CCD	APEXII CCD	APEXII CCD	APEXII CCD	APEXII CCD	APEXII CCD
Crystal size/mm^3	0.48 × 0.18 × 0.02	0.20 × 0.15 × 0.02	0.12 × 0.12 × 0.01	0.10 × 0.06 × 0.01	0.12 × 0.09 × 0.02	0.12 × 0.06 × 0.01	0.09 × 0.06 × 0.04
Crystal color; form	light-pink; plate	colorless; plate	colorless; fragment	colorless; plate	light-pink; plate	violet; plate	yellow; plate
Space group	P1	P1	P1	P1	P1	P1	P1
Formula units, Z	2	2	2	1	1	1	1
a/Å	4.9750(10)	5.0188(9)	4.9187(3)	5.4558(3)	5.5602(2)	5.495(3)	5.4297(7)
b/Å	5.4747(11)	5.6180(10)	5.2357(3)	7.3180(4)	7.4100(3)	7.394(4)	7.3308(9)
c/Å	13.603(3)	13.734(2)	12.8459(8)	8.3382(5)	8.4276(4)	8.330(5)	8.2795(10)
α/°	98.86(3)	99.254(3)	83.987(3)	100.231(2)	100.110(2)	100.604(15)	100.356(5)
β/°	93.63(3)	93.756(3)	81.286(3)	98.614(2)	98.578(2)	97.550(14)	98.088(5)
γ/°	99.09(3)	98.845(3)	80.117(3)	93.022(2)	92.744(2)	92.858(12)	92.982(5)
V/Å^3	360.02(13)	376.02(12)	321.09(3)	322.84(3)	337.03(2)	328.8(3)	319.95(7)
μ/mm^{-1}	10.966	11.648	14.054	10.399	10.808	11.379	11.869
X-ray Dens./g·cm^{-3}	3.190	3.562	3.592	3.035	3.058	3.155	3.241
Range θ_{min}–θ_{max}	3.87–30.00	3.02–31.06	3.96–30.98	3.79–41.89	2.80–41.52	2.81–31.00	2.53–36.71
Range h	−6→6	−7→7	−7→6	−10→10	−10→10	−7→7	−9→8
k	−7→3	−7→8	−7→7	−13→13	−13→14	−10→10	−12→12
l	−19→19	−19→19	−18→18	−15→15	−15→15	−12→11	0→13
Meas. refl.	4677	4430	7650	19986	17841	4582	3000
Indep. refl.	2087	2326	2011	4436	4843	2057	3000
Obs.refl. [$I > 2\sigma(I)$]	1831	1996	1600	3262	3767	1568	2566
R_i	0.0287	0. 0287	0.0461	0.0656	0.0285	0.0364	-
Abs. corr.	SADABS	SADABS	SADABS	SADABS	SADABS	SADABS	TWINABS
Trans. coef. T_{min}; T_{max}	0.526; 0.748	0. 443; 0.663	0.480; 0.747	0.531; 0.748	0.479; 0.748	0.592; 0.747	0.257; 0.439
Number of parameters	104	104	100	113	113	113	114
$R[F^2 > 2\sigma(F^2)]$	0.0332	0.0350	0.0380	0.0353	0.0264	0.0380	0.0387
$wR2(F^2$ all)	0.1053	0.0950	0.0994	0.0712	0.0538	0.0850	0.0880
Goof	1.1324	1.041	1.032	1.019	1.010	1.037	1.082
CSD number	1951017	1951013	1951019	1951015	1951016	1951014	1951018

2.3. Hydrogen Bonding Schemes

In contrast to the $M(H_2AsO_4)_2(H_3AsO_4)_2$ crystal structures where the localization of all hydrogen atoms and thus interpretation of the hydrogen bonds were unproblematic (Table 2), a clear assignment of the hydrogen bonding scheme was not possible for the $M(HAsO_4)(H_3AsO_4)(H_2O)_{0.5}$ and $Zn(HAsO_4)(H_3AsO_4)$ structures. Therefore, the bond valence method [9] was used to assign those O atoms in the three $M(HAsO_4)(H_3AsO_4)(H_2O)_{0.5}$ and $Zn(HAsO_4)(H_3AsO_4)$ structures that most probably carry a hydrogen atom. For all M^{II}–O bonds, the values of Brese and O'Keeffe [10] were applied, and for As^{V}–O bonds the values by Gangé and Hawthorne [11]. Results of the bond valence sum (BVS) calculations are listed in Table 1 and indicate the following atoms as the most probable donor groups, because they have the lowest bond valence sums (≤1.3 valence units) of all oxygen atoms: O1 bonded to As1, and O4, O6 and O8 bonded to As2. All other O atoms have considerably higher bond valence sums between 1.5 and 2.0 valence units.

In analogy with the crystal-chemical features of $M(H_2AsO_4)_2(H_3AsO_4)_2$ where the OH groups of the AsO_4 tetrahedra do not bond to the metal cations, all four assigned OH groups are bonded solely to arsenic as part of an AsO_4 tetrahedron and also show the longest As–O bonds in the two types of tetrahedra. Therefore, As1 represents a $HAsO_4^-$ anion and As2 the fully protonated acid, in accordance with charge neutrality of the overall structure. Analysis of the O···O distances around the four OH groups/(disordered) water molecules revealed hydrogen bonds with possible acceptor atoms listed in Table 2. This includes a very strong hydrogen bond between O4 and O2 with an O···O distance of ≈2.44 Å, and other strong hydrogen bonds between 2.60 and 2.65 Å for $D \cdots A$ contacts. The formation of these hydrogen bonds is also reflected in the BVS values of the acceptor O atoms that do not carry a hydrogen atom themselves. O2 and O5 are considerably undersaturated (BVS between 1.5 and 1.8 valence units) but are the acceptor atoms of the strongest hydrogen bonds (Table 2). On the other hand, oxygen atoms O3 and O7 are saturated with BVS values of 2.0 valence units and do not take part in any hydrogen bonding interaction. In case the water molecule is involved in hydrogen bonding, the hydrogen bonds become weaker ($D \cdots A$: 2.60–2.92 Å). The weakest hydrogen bond is developed in $Zn(HAsO_4)(H_3AsO_4)$ between O6 and O4 (3.07 Å), connecting two adjacent layers long [001]. Supposed hydrogen bonds for the $M(HAsO_4)(H_3AsO_4)(H_2O)_{0.5}$ and $Zn(HAsO_4)(H_3AsO_4)$ structures are illustrated in Figure 3. The various possibilities for hydrogen bonding in the two types of structures make it seem likely that parts of the hydrogen atoms are disordered and thus could not unambiguously be located in difference Fourier syntheses.

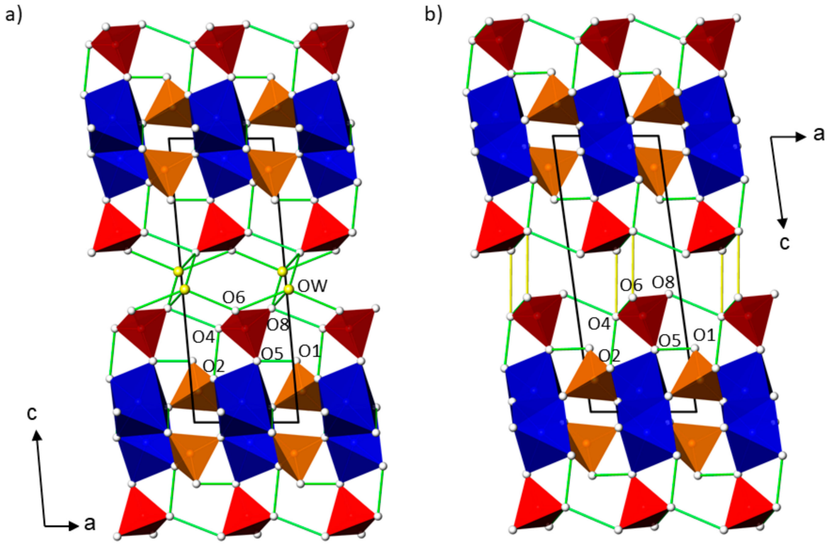

Figure 3. (**a**) Possible hydrogen bonding schemes in the crystal structures of $Mn(HAsO_4)(H_3AsO_4)(H_2O)_{0.5}$ ((a); projection along [010]) and $Zn(HAsO_4)(H_3AsO_4)$ ((**b**); projection along [010]). Hydrogen bonds with $D \cdots A$ contacts < 3.0 Å are given as green lines, and those > 3.0 Å as yellow lines. Color code as in Figure 2.

2.4. AsO_4 Tetrahedra in the Sructures

The averaged As–O bond lengths for each AsO_4 tetrahedron in the refined structures are collated in Table 1. Individual averaged values scatter only slightly (range 1.677 to 1.689 Å), and the overall mean of the 14 independent tetrahedral AsO_4 groups in the seven structures is 1.685 Å, a value in very good agreement with that of 1.687 Å reported in literature [12]. Very recently, a statistical evaluation of As–O bond lengths in AsO_4^{3-}, $HAsO_4^{2-}$, $H_2AsO_4^-$ and H_3AsO_4 groups was published [13], revealing the following average values: 1.667(18) Å for As–O bonds to nonprotonated O atoms, 1.728(19) Å for As–OH bonds in $HAsO_4^{2-}$ groups, 1.714 (12) Å for As–OH bonds in $H_2AsO_4^-$ groups and 1.694(16) Å for As–OH bonds in H_3AsO_4 groups. These values are in very good agreement with corresponding values for averaged As–OH bond lengths in the four $M(H_2AsO_4)_2(H_3AsO_4)_2$ structures: M = Mg, 1.698 Å for the H_3AsO_4 group and 1.714 Å for the $H_2AsO_4^-$ group; M = Mn, 1.695 and 1.710 Å; M = Co, 1.698 and 1.713 Å; M = Ni, 1.701 and 1.713 Å. On the other hand, comparison of the averaged As–OH bond lengths [13] with those of the assigned $HAsO_4^{2-}$ and H_3AsO_4 groups in the structures of $M(HAsO_4)(H_3AsO_4)(H_2O)_{0.5}$ and $Zn(HAsO_4)(H_3AsO_4)$ shows some subtle differences. Both literature values for As–OH in a $HAsO_4^{2-}$ (1.728(19) Å) and a H_3AsO_4 group (1.694(16) Å) are slightly larger than corresponding values in the three structures (Mn = 1.708, 1.688 Å; Cd = 1.714, 1.686 Å, Zn = 1.710, 1.686 Å). Nevertheless, individual values match the literature values within the single standard deviation of the latter. These slight differences might also indicate some disorder of the hydrogen atoms, as already suspected in Section 2.3.

2.5. Comparison of the Crystal Structures

For a quantitative comparison of the isotypic crystal structures within the $M(H_2XO_4)_2(H_3XO_4)_2$ series (M = Mg, Mn, Co, Ni, Cu; X = As, P) and between the two isotypic structures of $M(HAsO_4)(H_3AsO_4)(H_2O)_{0.5}$ (M = Mn, Cd), respectively, the program *compstru* [7] available at the Bilbao Crystallographic Server [14] was used. Due to different treatments of H atoms in the various refinements, e.g., by constrains/restrains regarding O–H bond lengths, the comparisons do not include hydrogen atoms.

$Zn(H_2AsO_4)_2(H_3AsO_4)_2$ was chosen as a reference to which all structures in the $M(H_2XO_4)_2(H_3XO_4)_2$ series were compared. As can be seen from the numerical details of the comparisons compiled in Table 4, the crystal structures of $Zn(H_2AsO_4)_2(H_3AsO_4)_2$ and its Mg, Co, and Ni analogues show a very high similarity ($\Delta < 0.02$) due to similar ionic radii of the four metal cations. Except for the Mg member for which data were recorded at −173 °C, all other crystals were measured at room temperature. The minor effect of the temperature on M–O and As–O bond lengths is neglected. Mn with its greater ionic radius leads to a somewhat larger difference ($\Delta = 0.033$). Likewise, substitution of the arsenate groups by smaller phosphate tetrahedra (Co–P) affects the displacements between comparable atomic pairs. Although individual displacement values reach up to 0.17 Å for some O atoms, Δ amounts to only 0.037 and thus indicates a high similarity of the two structures. The most remarkable change, however, pertains to the Cu member ($\Delta = 0.112$). Here the highest displacement is nearly 0.7 Å for atom O3 that represents the axially bound O atom in the MO_6 octahedron. Due to the Jahn–Teller effect associated with the copper(II) cation, the CuO_6 octahedron distorts under considerable elongation of the axial Cu–O3 bond.

The *compstru* program was also used to check the relationship between the $M(H_2XO_4)_2(H_3XO_4)_2$ structure type and the crystal structure of $CdH_{10}(AsO_4)_4$. The latter crystallizes likewise in space group $P-1$ with one formula unit, has the metal cation situated on an inversion center (Wyckoff position 1*a*) and exhibits similar lattice parameters, $a = 5.69(5)$, $b = 7.42(4)$, $c = 8.60(6)$ Å, $\alpha = 105.17(12)$, $\beta = 95.13(5)$, $\gamma = 91.85(8)°$ [4]. The evaluation of structural similarity revealed very large displacements between corresponding atomic pairs. For example, the two types of As atoms in the crystal structures have displacements of 1.71 and 1.97 Å, respectively, and for some oxygen atom displacements >2.0 Å were calculated. Hence the crystal structures of $CdH_{10}(AsO_4)_4$ and $M(H_2XO_4)_2(H_3XO_4)_2$ cannot be considered as isotypic, as already suggested in [5], but can be regarded as isopointal [15].

Comparison of the two isotypic $M(HAsO_4)(H_3AsO_4)(H_2O)_{0.5}$ structures again shows a high degree of similarity between them. Notable differences with displacements between 0.1 and 0.2 Å affect atom pairs O5 and O6 of the H_3AsO_4 tetrahedron, and the water molecule (Table 4).

Table 4. Numerical details from the comparisons of the crystal structure of $Zn(H_2AsO_4)_2(H_3AsO_4)_2$ [a] with isotypic structures in the $M(H_2XO_4)_2(H_3XO_4)_2$ series (*M* = Mg, Mn, Co, Ni, Cu; *X* = As, P), and between $Mn(HAsO_4)(H_3AsO_4)(H_2O)_{0.5}$ and $Cd(HAsO_4)(H_3AsO_4)(H_2O)_{0.5}$ using the *compstru* program [7].

$Zn(H_2AsO_4)_2(H_3AsO_4)_2$ *versus* $M(H_2AsO_4)_2(H_3AsO_4)_2$						
***M*1**	**Mg**	**Mn**	**(Co,P) [b]**	**(Co,As)**	**Ni**	**Cu [c]**
Atom, atomic displacement |u|/Å						
Zn1/*M*1	0	0	0	0	0	0
As1/As1(P1)	0.0111	0.0289	0.0746	0.0077	0.0200	0.3198
As2/As2(P2)	0.0176	0.0434	0.0852	0.0041	0.0122	0.1569
O1	0.0242	0.0737	0.1646	0.0134	0.0394	0.2641
O2	0.0241	0.0305	0.1641	0.0165	0.0285	0.3981
O3	0.0295	0.0500	0.1157	0.0272	0.0508	0.6942
O4	0.0253	0.0353	0.0889	0.0206	0.0184	0.2552
O5	0.0386	0.0497	0.1497	0.0185	0.0129	0.0974
O6	0.0230	0.0384	0.0669	0.0100	0.0337	0.2862
O7	0.0061	0.0807	0.1612	0.0051	0.0266	0.3203
O8	0.0295	0.0165	0.1616	0.0224	0.0308	0.3185
degree of lattice distortion (S)	0.0049	0.0078	0.0176	0.0030	0.0046	0.0243
arithmetic mean (d_{av})	0.0218	0.0426	0.1174	0.0139	0.0260	0.2963
measure of similarity (Δ)	0.014	0.033	0.037	0.017	0.011	0.112
$Mn(HAsO_4)(H_3AsO_4)(H_2O)_{0.5}$ *versus* $Cd(HAsO_4)(H_3AsO_4)(H_2O)_{0.5}$						
Atom, atomic displacement |u|/Å						
Mn1/Cd1	0.0576					
As1	0.0523					
As2	0.0816					
O1	0.0540					
O2	0.0835					
O3	0.0492					
O4	0.0645					
O5	0.1206					
O6	0.1899					
O7	0.0747					
O8	0.0497					
OW	0.1435					
degree of lattice distortion (S)	0.0095					
arithmetic mean (d_{av})	0.0851					
measure of similarity (Δ)	0.037					

[a] Lattice parameters: a = 5.460(2), b = Å 7.389(1), c = 8.347(1) Å, α =100.83(4), β = 97.90(4), γ = 92.89(3)°. [b] Standardized [16] lattice parameters: a = 5.286(2), b = 7.195(4), c = 8.121(4) Å, α = 101.10(4), β = 96.72(3), γ = 92.97(3)°. [c] Lattice parameters: a = 5.392(3) Å, b = 7.632(4) Å, c = 8.298(5) Å, α = 105.87(4)°, β = 97.63(3)°, γ = 93.6(1)°.

3. Materials and Methods

3.1. Synthesis and Crystal Growth

The chemicals used ($MnCO_3$, $CdCO_3$, ZnO, $Mg(OH)_2$, $CoCO_3{\cdot}xH_2O$, $NiCO_3$, H_3AsO_4) were of *pro analysi* quality. The target compounds were prepared by treating the corresponding metal carbonate, oxide or hydroxide with an excess of concentrated arsenic acid (80 wt %); the employed molar ratio H_3AsO_4:metal precursor was ≈10:1. The solid metal precursors were added in small portions to the acid and warmed (ca. 70 °C) until a clear solution was obtained overnight. In case the metal precursor dissolution was incomplete, the suspension was filtered through a G4 glass frit. All solutions were then left at room temperature in a desiccator filled with concentrated sulfuric acid until the first crystals appeared. The crystallization process lasted at least about one week; yields were not determined.

All grown crystals of the $M(H_2AsO_4)_2(H_3AsO_4)_2$ (M = Mg, Co, Ni) phases had a plate-like form and were directly taken out of the mother liquor. $Cd(HAsO_4)(H_3AsO_4)(H_2O)_{0.5}$ crystallized in form of thin plates and was the first crystallisation product from the solution. After a few days, these crystals converted in the mother liquor into coarse-crystalline $CdH_{10}(AsO_4)_4$ [4]. Likewise, $Mn(HAsO_4)(H_3AsO_4)(H_2O)_{0.5}$ crystals were the first crystallization product and converted over the course of a few days into $Mn(H_2AsO_4)_2(H_3AsO_4)_2$. $Zn(HAsO_4)(H_3AsO_4)$ crystals appeared with an unspecific form together with synthetic koritnigite ($ZnHAsO_4{\cdot}H_2O$ [17]; platy crystals). The amount of the latter phase increased in the remaining mother liquor over time.

3.2. *Single Crystal X-ray Diffraction*

Since all crystals appeared to be highly hygroscopic, they were immediately immersed in perfluorinated oil (Fomblin®Y, Sigma-Aldrich, Taufkirchen, Germany) and optically preselected under a polarizing microscope. The diffraction studies (Mo Kα radiation; Bruker SMART CCD or APEX-II CCD diffractometer; Bruker-AXS Inc. (Madison, WI, USA) followed standard procedures, including absorption corrections based on a multi-scan approach [18,19]. All crystal structures were solved with *SHELXT* [20] and refined with *SHELXL* [21]. The diffraction pattern of $Ni(H_2AsO_4)_2(H_3AsO_4)_2$ revealed a two-domain crystal (arbitrarily intergrown). Intensity data of this crystal were assigned to the two different domains and further processed as a HKLF-5 file; the ratio of the two domains refined to a value of 0.57:0.43. For better comparison, atomic coordinates and atom labels of all $M(H_2AsO_4)_2(H_3AsO_4)_2$ (M = Mg, Mn, Co, Ni) structures were finally adapted to the structure data of $Zn(H_2AsO_4)_2(H_3AsO_4)_2$ [6]. Likewise, the two new $M(HAsO_4)(H_3AsO_4)(H_2O)_{0.5}$ (M = Mn, Cd) structures are described with comparable atomic coordinates and atom labels. In this structure type, conspicuous electron density was observed around an inversion center after modelling the $M(HAsO_4)(H_3AsO_4)$ framework. This electron density was assigned to the O atom of a water molecule of crystallization, disordered around an inversion center. Because the symmetry-related water molecules cannot be occupied at the same time, the occupancy of the water molecule was constrained to 0.5. For the final model, this atom was refined with an isotropic displacement parameter. In the closely related structure of $Zn(HAsO_4)(H_3AsO_4)$, no such additional electron density was found.

For the $M(H_2AsO_4)_2(H_3AsO_4)_2$ (M = Mg, Mn, Co, Ni) crystal structures, all hydrogen atoms could clearly be located from difference Fourier syntheses. For refinement, their H–O distances were restrained to 0.90(1) Å, together with a common $U_{\mathrm{iso}}(H)$ parameter. For the crystal structures of $M(HAsO_4)(H_3AsO_4)(H_2O)_{0.5}$ (M = Mn, Cd) and $Zn(HAsO_4)(H_3AsO_4)$, an unambiguous assignment of hydrogen atoms was not possible. Hence, their positions are not included in the final models. Graphical representations of the crystal structures were performed with ATOMS for Windows [22].

Details of numerical values of the data collections and structure refinements are gathered in Table 3 and Supplementary Materials. Further details of the crystal structure investigations may be obtained from The Cambridge Crystallographic Data Centre (CCDC) on quoting the depository numbers listed at the end of Table 3. The data can be obtained free of charge via www.ccdc.cam.ac.uk/structures.

4. Conclusions

The oxidoarsenates(V) $M(H_2AsO_4)_2(H_3AsO_4)_2$ (M = Mg, Mn, Co, Ni), $M(HAsO_4)(H_3AsO_4)(H_2O)_{0.5}$ (M = Mn, Cd) and $Zn(HAsO_4)(H_3AsO_4)$ were crystallized from highly acidic solutions. The results of structure refinements of isotypic $M(H_2XO_4)_2(H_3XO_4)_2$ (M = Mg, Mn, Co, Ni; X = As) compounds from single crystal X-ray data supplement the knowledge on this structure type. Quantitative comparisons between all known crystal structures in this series with M = Mg, Mn, Co, Ni, Cu, Zn; X = As; P revealed a high similarity with the exception for the (Cu,As) member. The crystal structure of the latter shows considerable distortions due to the Jahn–Teller effect of Cu(II), leading to a displacement of up to 0.7 Å between related atomic pairs. It was also shown that the isoformular compound $CdH_{10}(AsO_4)_4$ (= $Cd(H_2AsO_4)_2(H_3AsO_4)_2$) is not isotypic with the $M(H_2XO_4)_2(H_3XO_4)_2$ series, but isopointal. The crystal structures of the two isotypic $M(HAsO_4)(H_3AsO_4)(H_2O)_{0.5}$ (M = Mn, Cd) compounds and of $Zn(HAsO_4)(H_3AsO_4)$ are closely related. They comprise of $M(HAsO_4)(H_3AsO_4)$ layers that are linked through hydrogen-bonded water molecules in the water-containing structures, or directly in the water-free structure. As–O distances in the two types of tetrahedra ($HAsO_4^{2-}$; H_3AsO_4) suggest disorder of the hydrogen atoms that could not be located in the present study.

Supplementary Materials: The following are available online at http://www.mdpi.com/2304-6740/7/10/122/s1, the CIFs and the checkCIF output files for $M(H_2AsO_4)_2(H_3AsO_4)_2$ (M = Mg, Mn, Co, Ni), $M(HAsO_4)(H_3AsO_4)(H_2O)_{0.5}$ (M = Mn, Cd) and $Zn(HAsO_4)(H_3AsO_4)$.

Funding: This research received no external funding.

Acknowledgments: The X-ray centre of the TU Wien is acknowledged for providing access to the single-crystal and powder X-ray diffractometers.

Conflicts of Interest: The author declares no conflict of interest.

References

1. Salmon, J.E.; Terrey, H. The systems zinc oxide–phosphoric oxide–water and manganous oxide–phosphoric oxide–water at temperatures between 25° and 100°. *J. Chem. Soc.* **1950**, 2813–2824. [CrossRef]
2. Herak, R.; Prelesnik, B.; Čurić, M.; Djurić, S. The crystal structure of $Co(H_2PO_4)_2{\cdot}2H_3PO_4$. *Z. Kristallogr.* **1983**, *164*, 25–30. [CrossRef]
3. Averbuch-Pouchot, M.T.; Durif, A. *Topics in Phosphate Chemistry*; World Scientific: Singapore, 1996; p. 346.
4. Boudjada, A.; Durif, A.; Guitel, J.C. Structure d'un orthoarsenate acide de cadmium: $CdH_{10}(AsO_4)_4$. *Acta Crystallogr. Sect. B* **1980**, *B36*, 133–135. [CrossRef]
5. Tran Qui, D.; Chiadmi, M. Structure de Décahydrogénotétraarsenate de Cuivre et Isotypie dans la Série $M^{II}H_{10}(AsO_4)_4$ (M^{II} = Mg, Mn, Co, Ni, Cu et Zn). *Acta Crystallogr. Sect. C* **1986**, *C42*, 391–393. [CrossRef]
6. Sure, S.; Guse, W. The crystal structure of zinc-decahydrogen-tetraarsenate $ZnH_{10}(AsO_4)_4$. *Neues Jahrb. Mineral. Monatsh.* **1989**, *9*, 401–409.
7. De la Flor, G.; Orobengoa, D.; Tasci, E.; Perez-Mato, J.M.; Aroyo, M.I. Comparison of structures applying the tools available at the Bilbao Crystallographic Server. *J. Appl. Crystallogr.* **2016**, *49*, 653–664. [CrossRef]
8. Shannon, R.D. Revised effective ionic radii and systematic studies of interatomic distances in halides and chalcogenides. *Acta Crystallogr. Sect. A* **1976**, *A32*, 751–767. [CrossRef]
9. Brown, I.D. *The Chemical Bond in Inorganic Chemistry: The Bond Valence Model*; Oxford University Press: Oxford, UK, 2002.
10. Brese, N.E.; O'Keeffe, M. Bond-valence parameters for solids. *Acta Crystallogr. Sect. B* **1991**, *B47*, 192–197. [CrossRef]
11. Gagné, O.C.; Hawthorne, F.C. Comprehensive derivation of bond-valence parameters for ion pairs involving oxygen. *Acta Crystallogr. Sect. B* **2015**, *B71*, 562–578. [CrossRef] [PubMed]
12. Gagné, O.C.; Hawthorne, F.C. Bond-length distributions for ions bonded to oxygen: Metalloids and post-transition metals. *Acta Crystallogr. Sect. B* **2018**, *B74*, 63–78. [CrossRef]
13. Schwendtner, K.; Kolitsch, U. Three new acid M^+ arsenates and phosphates with multiply protonated As/PO_4 groups. *Acta Crystallogr. Sect. C* **2019**, *C75*, 1134–1141. [CrossRef] [PubMed]
14. Aroyo, M.I.; Perez-Mato, J.M.; Capillas, C.; Kroumova, E.; Ivantchev, S.; Madariaga, G.; Kirov, A.; Wondratschek, H. Bilbao Crystallographic Server I: Databases and crystallographic computing programs. *Z. Kristallogr.* **2006**, *221*, 15–27. [CrossRef]
15. Lima-de-Faria, J.; Hellner, E.; Liebau, F.; Makovicky, E.; Parthé, E. Nomenclature of inorganic structure types. Report of the International Union of Crystallography Commission on Crystallographic Nomenclature Subcommittee on the Nomenclature of Inorganic Structure Types. *Acta Crystallogr. Sect. A* **1990**, *A46*, 1–11. [CrossRef]
16. Gelato, L.M.; Parthé, E. STRUCTURE TIDY—A computer program to standardize crystal structure data. *J. Appl. Crystallogr.* **1987**, *20*, 139–143. [CrossRef]
17. Keller, P.; Hess, H.; Riffel, H. Die Kristallstruktur von Koritnigit, $Zn[H_2O|HOAsO_3]$. *Neues Jahrb. Mineral. Abh.* **1980**, *138*, 316–332.

18. Krause, L.; Herbst-Irmer, R.; Sheldrick, G.M.; Stalke, D. Comparison of silver and molybdenum microfocus X-ray sources for single-crystal structure determination. *J. Appl. Crystallogr.* **2015**, *48*, 3–10. [CrossRef] [PubMed]
19. Sheldrick, G.M. *TWINABS*; University of Göttingen: Göttingen, Germany, 2012.
20. Sheldrick, G.M. SHELXT—Integrated space-group and crystal-structure determination. *Acta Crystallogr. Sect. A* **2015**, *A71*, 3–8. [CrossRef] [PubMed]
21. Sheldrick, G.M. Crystal structure refinement with *SHELXL*. *Acta Crystallogr. Sect. C* **2015**, *C71*, 3–8.
22. Dowty, E. Atoms *for Windows*, Version 6.3; Shape Software: Kingsport, TN, USA, 2006.